

**Aerosol  
microphysical  
retrievals from PFR  
and AERONET**

S. Kazadzis et al.

# Aerosol microphysical retrievals from Precision Filter Radiometer direct solar radiation measurements and comparison with AERONET

S. Kazadzis<sup>1</sup>, I. Veselovskii<sup>2</sup>, V. Amiridis<sup>3</sup>, J. Gröbner<sup>4</sup>, A. Suvorina<sup>2</sup>, S. Nyeki<sup>4</sup>, E. Gerasopoulos<sup>1</sup>, N. Kouremeti<sup>4</sup>, M. Taylor<sup>1</sup>, A. Tsekeri<sup>3</sup>, and C. Wehrli<sup>4</sup>

<sup>1</sup>Institute for Environmental Research and Sustainable Development (IERSD), National Observatory of Athens (NOA), Metaxa & Vas Pavlou, Penteli, 15236, Athens, Greece

<sup>2</sup>Physics Instrumentation Center, Moscow, Russia

<sup>3</sup>Institute for Astronomy, Astrophysics, Space Applications and Remote Sensing (IAASARS), National Observatory of Athens (NOA), Metaxa & Vas. Pavlou, Penteli, 15236, Athens, Greece

<sup>4</sup>Physikalisch-Meteorologisches Observatorium Davos, World Radiation Center – PMOD/WRC, Davos, Switzerland

Received: 4 December 2013 – Accepted: 6 December 2013 – Published: 10 January 2014

Correspondence to: S. Kazadzis (kazadzis@noa.gr)

Published by Copernicus Publications on behalf of the European Geosciences Union.

Title Page

Abstract

Introduction

Conclusions

References

Tables

Figures

⏪

⏩

◀

▶

Back

Close

Full Screen / Esc

Printer-friendly Version

Interactive Discussion

## Abstract

Synchronized sun-photometric measurements from the AERONET-CIMEL and GAW-PFR aerosol networks are used to compare retrievals of the aerosol optical depth, effective radius and volume concentration during a high temporal resolution measurement campaign at the Athens site in the Mediterranean Basin from 14–22 July 2009. During this period, direct sun AOD retrievals from both instruments exhibited small differences in the range 0.01–0.02 despite the presence of a strong dust event. In addition to AERONET-CIMEL inversion data, an independent inversion method was applied that involves expanding the particle size distribution in terms of measurement kernels so as to estimate bulk particle parameters from a linear-estimated combination of the input optical data. AOD measurements obtained from both CIMEL and PFR instruments using this method also showed reasonable agreement. For low aerosol loads ( $\text{AOD} < 0.2$ ), measurements of the effective radius by the PFR were found to be  $-20\%$  to  $+30\%$  different from CIMEL values for both direct sun data and inversion data. At higher loads ( $\text{AOD} > 0.4$ ), measurements of the effective radius by the PFR are consistently  $20\%$  lower than CIMEL for both direct sun and inversion data. Volume concentrations at low aerosol loads from the PFR are up to  $80\%$  higher than the CIMEL for direct sun data, but inversion data suggests that volume concentrations from the PFR are up to  $20\%$  lower than the CIMEL under these same conditions. At higher loads, the percentage difference in volume concentrations from the PFR and CIMEL is systematically negative with inversion data predicting differences  $30\%$  lower than those obtained from direct sun data. An assessment of the effect of errors in the AOD retrieval on the estimation of PFR bulk parameters was made using Monte Carlo simulations and demonstrated that it is possible to estimate the effective radius with an uncertainty below  $60\%$  and the volume concentration with an uncertainty below  $65\%$  even when  $\text{AOD} < 0.2$  and when the input errors are as high as  $10\%$ .

## Aerosol microphysical retrievals from PFR and AERONET

S. Kazadzis et al.

Title Page

Abstract

Introduction

Conclusions

References

Tables

Figures

⏪

⏩

◀

▶

Back

Close

Full Screen / Esc

Printer-friendly Version

Interactive Discussion



## Aerosol microphysical retrievals from PFR and AERONET

S. Kazadzis et al.

Title Page

Abstract

Introduction

Conclusions

References

Tables

Figures

⏪

⏩

◀

▶

Back

Close

Full Screen / Esc

Printer-friendly Version

Interactive Discussion



## Highlights

- A comparison of high temporal resolution synchronous CIMEL and PFR direct sun AOD measurement retrievals
- Calculation of bulk aerosol microphysics parameters using a linear estimation inversion technique
- A comparison of retrieved aerosol volume concentrations and effective radii from CIMEL and PFR inversions
- An analysis of the sensitivity of PFR retrievals to random errors on the optical input data

## 1 Introduction

The quantification of aerosol properties and their spatial and temporal variability is crucial in order to define their forcing effect on climate. Since this has not yet been done effectively, the uncertainty of the impact of aerosols is very large, especially with respect to global warming resulting from the forcing effect of greenhouse gases (Hansen et al., 2005; IPCC, 2007). More specifically, aerosols exert a direct forcing on climate by reflecting or absorbing incoming sunlight, and an indirect forcing on climate by altering cloud properties and precipitation. However, it is not possible to quantify both forcing effects to the required accuracy if the microphysical properties of aerosols (i.e. size, shape, and chemical composition) and their interaction with clouds are not described adequately (Mischenko et al., 2007).

Although the spatial and temporal resolution required for global studies of the effect of aerosols on climate can only be effectively achieved through satellite observations (Hansen et al., 1997), ground-based observations play an important role in aerosol monitoring and the validation of satellite retrievals. One of the most prominent ground-based networks is the AErosol ROBotic NETwork (AERONET). AERONET is

**Aerosol  
microphysical  
retrievals from PFR  
and AERONET**

S. Kazadzis et al.

Title Page

Abstract

Introduction

Conclusions

References

Tables

Figures

◀

▶

◀

▶

Back

Close

Full Screen / Esc

Printer-friendly Version

Interactive Discussion

a network of CIMEL sun-photometers which measure atmospheric aerosol properties (Holben et al., 1998). Numerous studies have been published using different aerosol related parameters derived from AERONET in the past two decades, establishing it as a worldwide recognized source of information about particle properties. Measurements of sun and sky radiances at a number of fixed wavelengths within the visible and near-infra red spectrum are performed, and advanced retrieval algorithms for microphysical aerosol properties have been developed in the framework of AERONET (e.g. Dubovik and King, 2000).

Another ground-based network, the Global Atmospheric Watch (GAW) network operated since 1999 by the World Optical Depth Research and Calibration Center (WORCC), is based at the World Radiation Center of the World Meteorological Organization (WMO) at Davos, Switzerland. Under the auspices of the WORCC, 12 existing GAW stations were chosen for the deployment and operation of a corresponding number of 12 Precision Filter Radiometers (PFR) (Wehrli, 2005).

Compared to the AERONET-CIMEL sun and sky-scanning photometer, the GAW-PFR as a classic sun-photometer, provides more limited optical data and the inversion of the retrieval of the full-set of the particle microphysical properties is, as a result, an ill-posed problem. For many applications though, it is sufficient to retrieve bulk aerosol properties such as the volume concentration ( $V_c$ ) and the effective radius ( $R_{\text{eff}}$ ) of the particle size distribution. These parameters are appropriate to use in radiation studies (instead of for example the number concentration and the mean radius) since they are more sensitive to the radiative properties of the particles (Hansen and Travis, 1974; Bohren and Huffman, 1983). Although an estimation of the  $V_c$  and  $R_{\text{eff}}$  alone is not adequate to accurately quantify the effect of aerosols on climate, they provide important information which can be used in validation studies of more complete retrieval schemes.

In this study, direct solar radiation measurements of PFR are used to estimate  $V_c$  and  $R_{\text{eff}}$  of the associated particle size distribution. This is motivated by recent results whereby particle bulk parameters were estimated from multi-wavelength

**Aerosol  
microphysical  
retrievals from PFR  
and AERONET**

S. Kazadzis et al.

Title Page

Abstract

Introduction

Conclusions

References

Tables

Figures

◀

▶

◀

▶

Back

Close

Full Screen / Esc

Printer-friendly Version

Interactive Discussion



measurements with LIDAR data inversion (Veselovskii et al., 2012). The aerosol optical depth (AOD) measurements used here, although having different information content to LIDAR measurements are known to be able to provide satisfactory estimates of  $V_c$  and  $R_{\text{eff}}$  and the inversion approach is based on an expansion of the particle size distribution in terms of measurement kernels (Twomey, 1977; Thomason and Osborn, 1992; Donovan and Carswell, 1997; Veselovskii et al., 2012). In this framework, the bulk particle parameters are estimated from a linear combination of input optical data we refer to this method as the “linear estimation” (LE) technique.

## 2 Instrumentation and methods

In order to harmonize the AERONET-CIMEL and GAW-PFR networks, calibration and intercomparison activities have been initiated. We report on one such activity that was coordinated in Athens, Greece during the period 14–22 July 2009. The LE method was applied to datasets from both networks and the  $V_c$  and  $R_{\text{eff}}$  of the size distribution were estimated along with an assessment of the effect of instrumental errors on the uncertainty on the retrieval. Furthermore, the results are compared with AERONET inversion products in order to assess the capabilities of the LE technique.

### 2.1 Aerosol sun-photometric measurements

A PFR travelling standard from the WORCC was located at the aerosol monitoring station of the Institute for Astronomy, Astrophysics, Space Applications and Remote Sensing (IAASARS) at the National Observatory of Athens (NOA), 191 m a.s.l. The station (shown in Fig. 1) is located in a sub-urban area, 3 km from the centre of Athens where IAASARS/NOA also operates a CIMEL sun-photometer as part of AERONET since 2008.

Measurements by the PFR travelling standard were taken at 1 min intervals and were evaluated according to GAW-PFR Level 3 data standards. According to this standard,

## Aerosol microphysical retrievals from PFR and AERONET

S. Kazadzis et al.

Title Page

Abstract

Introduction

Conclusions

References

Tables

Figures

◀

▶

◀

▶

Back

Close

Full Screen / Esc

Printer-friendly Version

Interactive Discussion

data is: (i) cloud-screened, (ii) manually-inspected, and (iii) pre-calibrated without a post-field campaign calibration (further details can be found on the WORCC homepage at: [www.pmodwrc.ch/worcc/](http://www.pmodwrc.ch/worcc/) under the menu “AOD QC/Calibration”). Measurements by the CIMEL sun-photometer were run according to the standard AERONET protocol whereby the measurement frequency depends on the optical air mass and time of day. In practice, AOD measurements are available every 10–11 min during low sun elevations and are available in near-real-time from the AERONET website. Level 2 AOD data obtained from the AERONET Version 2 Direct Sun Algorithm was collected. AERONET Level 2 data is: (i) pre- and post-field calibrated, (ii) automatically cloud-screened, and (iii) manually-inspected (further details concerning AERONET data processing procedures for AOD retrievals can be found at: [http://aeronet.gsfc.nasa.gov/new\\_web/data\\_description\\_AOD\\_V2.html](http://aeronet.gsfc.nasa.gov/new_web/data_description_AOD_V2.html)) and those related to inversion products at: [http://aeronet.gsfc.nasa.gov/new\\_web/Documents/Inversion\\_products\\_V2.pdf](http://aeronet.gsfc.nasa.gov/new_web/Documents/Inversion_products_V2.pdf).

## 2.2 Microphysical retrievals

The AERONET retrieval provides a large number of aerosol microphysical and optical properties. In particular, the volume size distribution is retrieved in 22 logarithmically equidistant radial ( $r$ ) bins in the size range  $0.05 \mu\text{m} \leq r \leq 15 \mu\text{m}$ . The real ( $m_R$ ) and imaginary part ( $m_I$ ) of the complex refractive index ( $m$ ) (where  $1.33 \leq m_R \leq 1.6$  and  $0.0005 \leq m_I \leq 0.5$ ) are retrieved for wavelengths corresponding to sky radiance measurements. In addition, the retrieval provides the following standard parameters for the total and the fine and course aerosol modes of the size distribution:  $V_c$  ( $\mu\text{m}^3 \mu\text{m}^{-2}$ ),  $\text{Reff}$  ( $\mu\text{m}$ ) and the volume median radius (not considered here).

The number of CIMEL sky radiance scans are normally limited to typically one scan per hour. In addition, the accuracy of the particle property retrieval is lower at high solar zenith angles (sza) and low AOD (Dubovik and King, 2000). As a result of these constraints, a significant proportion of AERONET measurements is excluded from the Level 2 product. On the contrary, direct sun measurements are performed at higher

temporal resolution (typically 10 min) and our aim here is to assess also their utility for deriving bulk measures of aerosol microphysics.

The retrieval of  $V_c$  and  $R_{\text{eff}}$  of the particle size distribution using the LE technique is described in detail in Veselovskii et al. (2012). Here we provide just the main steps of the inversion procedure. The input vector  $\mathbf{g}$  contains the input optical data (the spectrum of aerosol extinction) and is related to the volume size distribution  $\mathbf{v}$  as follows:

$$\mathbf{K}\mathbf{v} = \mathbf{g} \quad (1)$$

with  $\mathbf{K}$  being the matrix containing the discretized volume kernels (as rows). Any bulk particle property  $\mathbf{p}$  (e.g.  $V_c$  or  $R_{\text{eff}}$ ) can be estimated from Eq. (1):

$$\mathbf{p} = \mathbf{P}\mathbf{v} = \mathbf{P}\mathbf{K}^T(\mathbf{K}\mathbf{K}^T)^{-1}\mathbf{g} \quad (2)$$

where  $\mathbf{P}_{i,k}$  is a matrix containing the weight coefficients of different integral properties in each row  $i$ . For example, for volume ( $i = 1$ ), surface ( $i = 2$ ) and number concentrations ( $i = 3$ ):  $P_{1k} = 1$ ,  $P_{2k} = \frac{3}{r_k}$  and  $P_{3k} = \frac{3}{4\pi r_k^3}$  respectively. It should be mentioned that when retrieving  $\mathbf{p}$ , we consider only the projection of  $\mathbf{p}$  on the measured set  $\mathbf{g}$  and ignore the residual  $\mathbf{p}_\perp$  that can not be measured directly with the available set of observations  $\mathbf{g}$  (the so called “null-space”). For the retrieval of  $V_c$  and  $R_{\text{eff}}$  from AOD measurements, this is not expected to introduce large uncertainties since the measurements depend strongly on the parameters retrieved and the residual  $\mathbf{p}_\perp$  is therefore small. An estimation of the uncertainties introduced due to the null space is provided in Sect. 3.3.

The inverse problem in this formulation is under-determined (i.e. the set of input optical data measurements is limited and is generally not sufficient to obtain a unique solution). Moreover, the volume kernels  $\mathbf{K}$  depend on the size range of the size distribution and also upon the refractive index  $m$  which are both unknowns in the formulation. One way to overcome these constraints is to perform inversions for a set of different radial size ranges  $r$  and refractive indices  $m$  in the form of a “look-up table”. To be more

## Aerosol microphysical retrievals from PFR and AERONET

S. Kazadzis et al.

Title Page

Abstract

Introduction

Conclusions

References

Tables

Figures

◀

▶

◀

▶

Back

Close

Full Screen / Esc

Printer-friendly Version

Interactive Discussion



specific, we consider a set of inversion windows  $[r_{\min}, r_{\max}]$  in the range 0.075–10  $\mu\text{m}$  and a set of refractive indices whose real part  $m_{\text{R}}$  is in the range 1.35–1.65 and whose imaginary part  $m_{\text{I}}$  is in the range 0–0.02. Thus, instead of a single solution, we obtain a family of solutions and the selection is performed based on the resulting discrepancy as described in Veselovskii et al. (2012). The discrepancy  $\rho$  is defined as the difference between the measured data  $g_{\text{p}}$  and the calculated data  $\tilde{g}_{\text{p}}$  from the solution obtained. In the LE technique, we obtain  $N$  estimates of  $\tilde{g}_{\text{p}}$ , using for each one,  $N - 1$  measurements from the measured data  $g_{\text{p}}$  as suggested in (De Graaf et al. 2010);  $\rho$  is then calculated using the expression:

$$\rho = \sqrt{\frac{\sum_{\text{p}}^N (g_{\text{p}} - \tilde{g}_{\text{p}}(m))^2}{N}}. \quad (3)$$

The solutions are then sorted in accordance with their discrepancy from the minimal to maximal values and the bottom 1 % of solutions near the minima of the discrepancy are averaged to produce the final solution. It should be mentioned that the AOD, in contrast to the aerosol backscattering coefficient used in the study of Veselovskii et al. (2012), is not very sensitive to the refractive index  $m$  and hence decreases errors arising from a possibly incorrect choice of  $m_{\text{R}}$  and  $m_{\text{I}}$  windows. Further discussion on the uncertainties associated with the retrieval is provided in Sect. 3.3.

### 3 Results and discussion

#### 3.1 Aerosol variability during the experiment

The AOD at 440 nm and the Ångström Exponent (AE) at 412–870 nm from GAW-PFR measurements during the study period are presented in Fig. 1. Both the AOD and the AE show high variability. This is because the Mediterranean Basin is under the

**Aerosol  
microphysical  
retrievals from PFR  
and AERONET**

S. Kazadzis et al.

Title Page

Abstract

Introduction

Conclusions

References

Tables

Figures

⏪

⏩

◀

▶

Back

Close

Full Screen / Esc

Printer-friendly Version

Interactive Discussion







## Aerosol microphysical retrievals from PFR and AERONET

S. Kazadzis et al.

Title Page

Abstract

Introduction

Conclusions

References

Tables

Figures

⏪

⏩

◀

▶

Back

Close

Full Screen / Esc

Printer-friendly Version

Interactive Discussion

Further statistics on coincident AE showed a reasonable agreement between CIMEL and PFR mean values, calculated to be 1.44 and 1.52, respectively. When comparing coincident values it should be noted that the AE may depend on the number of wavelength channels used and also on the wavelengths themselves. Both CIMEL and PFR use 4 wavelengths but slightly different wavelength ranges of 440 to 870 nm, and 368 to 862 nm, respectively. More detail on the AOD differences is presented in Fig. 3.

The scatter varies between  $-0.035$  to  $0.01$  for 500 nm and  $-0.01$  to  $0.01$  for 865 nm with the variation on any particular day being between 0.01 and 0.02 (similar to the quoted AOD uncertainty of 0.015 for both instruments). The offset bias at Athens-NOA is  $-0.01$  and  $-0.001$  at 500 nm and 865 nm respectively. At both wavelengths, the Pearson product-moment correlation coefficients are very high ( $> 0.99$ ) and the calculated slopes are 0.99 and 1.04 at 500 nm and 865 nm respectively. The best-fit line is of high accuracy as individual outliers have a lower weighting in the LE model.

The quality of AOD data from the inter-comparison can be gauged by applying the WMO criteria discussed in WMO GAW report number 162 (WMO, 2005). According to these criteria, the ability to trace the calibration to a primary reference (“traceability”), is not currently possible based on physical measurement systems. The WMO report states that the initial form of traceability should be based on difference criteria such that an inter-comparison or co-location traceability is established if the AOD difference between networks is within specified limits. In the first instance, the definition of these limits depends on the method of measurement used. For finite field-of-view instruments such as the PFR and CIMEL, the limit (“U95”) is defined as follows for air mass,  $m$ :

$$U95 < \pm(0.005 + 0.010/m) \quad (4)$$

The first term accounts for instrumental and algorithmic uncertainties while the second term represents the uncertainty in the exo-atmospheric calibration value. The latter corresponds to a requirement for the relative uncertainty in the calibration of  $< 1\%$ . Figure 4 illustrates the AOD differences as a function of air mass. At 500 nm, almost

half of the data fall outside the WMO limits. The 865 nm channel was traceable with almost 99% of the data points fulfilling the current GAW criterion.

It is important to note that a lower AOD limit exists beyond which the AOD difference is difficult to minimize. An AOD inter-comparison study conducted by McArthur et al. (2003) compared network PFR and CIMEL sun-photometers against other AOD instruments. It was demonstrated that only a marginal improvement in AOD uncertainty at the 0.005 level was obtainable and requires further advances in the following areas: (i) solar pointing, (ii) better determination of Rayleigh reflectance, Ozone and other species' contributions to optical depth, and (iii) better instrument characterization (including calibration).

### 3.2.2 Effective radius, $R_{\text{eff}}$

The AOD datasets from both PFR and CIMEL were used as inputs in the LE method to calculate the  $V_c$  and  $R_{\text{eff}}$  of the particle size distribution. We performed a comparison of the results in order to assess possible differences. In addition, a third dataset, the AERONET sky radiance inversion product is also used for comparison of the results from the PFR and CIMEL LE retrievals. The three different methods used in our analysis are therefore as follows:

1. LE method with AOD data from the PFR (PFR-LE),
2. LE method with AOD data from the CIMEL (AERONET-LE),
3. AERONET Version 2 inversion products (AERONET Inv); Level 2 when available and Level 1.5 otherwise.

An example for the LE retrievals is shown in Fig. 5, where the expected anti-correlation between  $R_{\text{eff}}$  and AE is observed.

Time series of the  $R_{\text{eff}}$  retrieved by the above three methods is presented in Fig. 6. A generally good agreement between the PFR-LE and AERONET-LE derived values of  $R_{\text{eff}}$  is found (both in terms of absolute values and also temporal structure). On the days

## Aerosol microphysical retrievals from PFR and AERONET

S. Kazadzis et al.

Title Page

Abstract

Introduction

Conclusions

References

Tables

Figures



Back

Close

Full Screen / Esc

Printer-friendly Version

Interactive Discussion



## Aerosol microphysical retrievals from PFR and AERONET

S. Kazadzis et al.

Title Page

Abstract

Introduction

Conclusions

References

Tables

Figures

◀

▶

◀

▶

Back

Close

Full Screen / Esc

Printer-friendly Version

Interactive Discussion

having prominent bimodal distributions (see Fig. 2, 17–20 July) the PFR-LE method seems to slightly underestimate the respective values derived from the AERONET-LE method. The AERONET inversion code-derived values (“AERONET Inv”) of  $R_{\text{eff}}$  also show a reasonable agreement with respect to the overall baseline trend given the restrictions of the inversion. Moreover, at high solar zenith angles (sza), it can be seen that the inversion code provides higher  $R_{\text{eff}}$  values than the AERONET-LE calculated one.

In order to investigate sources of discrepancy between the different techniques, the difference between the PFR-LE and AERONET-LE -derived  $R_{\text{eff}}$  values is plotted vs. the sza and the AOD. For both direct sun measurements and the inversion data the percentage difference shows a general increase when the  $\text{sza} \approx 65\text{--}70^\circ$  (Fig. 7a). From a fairly constant absolute difference in the range 0 to  $-20\%$  ( $-7 \pm 14\%$  mean and standard deviation) scatter in the direct sun data increases to as much as 60% for  $\text{sza} > 70^\circ$ . A similar pattern is revealed with respect to the AERONET inversion data where the respective mean is  $-15 \pm 23\%$  (or  $-15 \pm 11\%$  for  $\text{sza} < 70^\circ$ ). The same differences are then plotted as a function of AOD (Fig. 7b).

For low aerosol loads where  $\text{AOD} < 0.2$ , the percentage difference between the  $R_{\text{eff}}$  obtained from the PFR and CIMEL is mostly positive, reaching a maximum of  $\approx 60\%$  for both direct sun and inversion data. For higher AOD loads, two distinct regions are discernable. In the range  $0.2 \leq \text{AOD} \leq 0.4$ , the percentage difference between the PFR and the CIMEL shows a significant spread and is mostly negative for both direct sun measurements (0 to  $-20\%$ ) and inversion data. The PFR data is predicting lower values of  $R_{\text{eff}}$  compared to the CIMEL of the order of 10% and 20% for the LE and inversion methods respectively. At moderate to high loads ( $\text{AOD} > 0.4$ ), the effect of PFR predicting lower  $R_{\text{eff}}$  values continues, but the percentage difference converges on a narrow band centered at  $-20\%$ .

### 3.2.3 Volume concentration, $V_c$

$V_c$  was also retrieved using the above three methods and the time series are shown in Fig. 8.

The agreement between the  $V_c$  from the PFR-LE and the AERONET-LE methods is quite good (both in terms of variability and absolute values). The AERONET inversion also echoes well the timing of the peaks, but is systematically much higher. This overestimation peaks during the period of elevated aerosol load due to the presence of a mixture of fine and coarse particles.

Investigating the percentage differences for the three different approaches as a function of AERONET AOD at 440 nm in Fig. 9 shows that the percentage difference between the PFR and CIMEL measurements of  $V_c$  tend to converge on the values  $-5\%$  and  $-50\%$  respectively at moderate to high AODs ( $> 0.4$ ). The two LE methods agree well (to within about  $-5\%$ ) when direct sun data is used and when the aerosol load is greater than 0.4. At lower aerosol loadings, the PFR-derived  $V_c$  appears higher by approximately  $20\%$ . The situation is reversed with AEROVET inversion data for which the percentage difference with PFR-LE tends to steadily increase with increasing AOD stabilising at around  $-50\%$  for  $AOD > 0.4$ .

### 3.3 Uncertainties of the retrieval

One of the basic issues when a new inversion technique is considered is a realistic estimation of uncertainties related to the retrieval of particle parameters. As was shown by Veselovskii et al. (2012), in the absence of input errors the uncertainties of the retrieval are due to the null-space and the unknown value of the refractive index  $m$ . It should be mentioned that the AOD is not very sensitive to  $m$  which, on the one hand has the desired effect of decreasing corresponding errors, but on the other hand deprives one of the possibility of estimating the value of  $m$  from measurements. Nevertheless, the presence of random errors in the input data induces additional uncertainties to the retrieval. To estimate the effect of such input errors we performed a numerical

Title Page

Abstract

Introduction

Conclusions

References

Tables

Figures

⏪

⏩

◀

▶

Back

Close

Full Screen / Esc

Printer-friendly Version

Interactive Discussion



simulation whereby synthetic optical data corresponding to four measurement channels of the PFR was computed from a bimodal particle size distribution (PSD) of the form:

$$\frac{dn(r)}{d\ln(r)} = \sum_{i=f,c} \frac{N_i}{(2\pi)^{1/2} \ln \sigma_i} \exp \left[ -\frac{(\ln r - \ln r_i)^2}{2(\ln \sigma_i)^2} \right]. \quad (5)$$

with  $N_i = N_{f,c}$  being the particle number density in the fine ( $f$ ) and the coarse ( $c$ ) mode. Each mode is represented by a lognormal distribution with modal radius  $r_{f,c}$  and dispersion  $\ln \sigma_{f,c}$ . In our simulations, we used two types of size distribution having the parameterisation listed in Table 1. The fine and coarse modes have modal radii  $r_f = 0.1 \mu\text{m}$  and  $r_c = 1 \mu\text{m}$  respectively but an equal dispersion  $\ln \sigma_f = 0.4$  and  $m = 1.45 - i \cdot 0.005$  were assumed for both modes. The Type I distribution ( $N_f/N_c = 10^4$ ) represents the situation when the fine mode is dominating the PSD while the Type II distribution ( $N_f/N_c = 10^2$ ) corresponds to a PSD with the coarse mode prevailing.

The uncertainty of the AOD measurements is about 0.02 for both the PFR and AERONET instruments thus, for an AOD value of 0.2, the relative error can be up to 10%. In addition, the errors in long wavelength channels can be higher than short wavelength channels since the corresponding AODs are also lower. In the somewhat idealized and simplified simulation presented here, we assumed that the uncertainties in all measurement *channels* are equivalent. To evaluate the effect of input uncertainties, random errors in the range of  $[0, \pm \varepsilon]$  were added to the PFR data and from this distorted optical data, particle parameters were retrieved. To increase the sample, the procedure was repeated 1000 times as a bootstrap thus allowing for more robust statistics. The results are presented in the form of cumulative probability distributions in Fig. 10.

Simulations were performed for  $\varepsilon = 5\%$  and  $\varepsilon = 10\%$ . For every value of  $\varepsilon_v$  the plot gives the probability that the retrieval uncertainty is below this quoted value. For example, it is concluded for the Type I distribution that in 90% of the cases, the uncertainty of the  $V_c$  estimation is below  $\varepsilon_v \approx 15\%$  and 25% for input errors  $\varepsilon = 5\%$  and 10%,

**Aerosol  
microphysical  
retrievals from PFR  
and AERONET**

S. Kazadzis et al.

Title Page

Abstract

Introduction

Conclusions

References

Tables

Figures

⏪

⏩

◀

▶

Back

Close

Full Screen / Esc

Printer-friendly Version

Interactive Discussion





are up to 20 % lower than the CIMEL. Higher aerosol loads were found to not rectify this situation. For AOD > 0.4, the percentage difference in  $V_c$  from the PFR and CIMEL is systematically negative with inversion data predicting differences 30 % lower than those obtained from direct sun data.

The use of the LE method in both CIMEL and PFR AOD measurements showed reasonable agreement. However, this study shows that implementation of such results to direct sun instruments requires the use of highly accurate AOD data since small AOD differences can have a sizeable impact on the calculated values of  $R_{\text{eff}}$  and  $V_c$ . The calculation of these bulk parameters by the LE method show an under-estimation as compared with AERONET inversions, with the highest differences being observed for AOD < 0.2 and for  $\text{sza} > 70^\circ$ . Despite the observed differences, the use of the LE method with direct sun sun-photometer data offers a number of advantages including:

- a. providing a unique opportunity to expand spatially the global data set of bulk aerosol properties ( $R_{\text{eff}}$  and  $V_c$ ) by using GAW-PFR network data in conjunction with other direct sun (AOD measuring) instruments,
- b. providing a unique opportunity to collect high temporal resolution time series data of bulk particle parameters by using AERONET or other instruments' AOD measurements which can be provided or already exist in various aerosol databases with a frequency of 1–15 min.

*Acknowledgements.* M. Taylor was supported by a Marie-Curie IEF funded project “AEROMAP: Global mapping of aerosol properties using neural network inversions of ground and satellite based data”, CN: 300515. S. Kazadzis’s work is supported by the Project (FP7-PEOPLE-2009-RG Marie Curie European Reintegration Grant, PERG-GA-2009-256391).

## References

Bohren, C. F. and Huffman, D. R.: Absorption and Scattering of Light by Small Particles, John Wiley, Hoboken, NJ, 1983.

## Aerosol microphysical retrievals from PFR and AERONET

S. Kazadzis et al.

Title Page

Abstract

Introduction

Conclusions

References

Tables

Figures



Back

Close

Full Screen / Esc

Printer-friendly Version

Interactive Discussion



## Aerosol microphysical retrievals from PFR and AERONET

S. Kazadzis et al.

Title Page

Abstract

Introduction

Conclusions

References

Tables

Figures

◀

▶

◀

▶

Back

Close

Full Screen / Esc

Printer-friendly Version

Interactive Discussion

De Graaf, M., Donovan, D., and Apituley, A.: Aerosol microphysical properties from inversion of tropospheric optical Raman lidar data, *Proceedings of ISTP 8, S06–O08, 19–23 October 2010, Delft, the Netherlands, 2010.*

Donovan, D. and Carswell, A.: Principal component analysis applied to multiwavelength lidar aerosol backscatter and extinction measurements, *Appl. Optics*, 36, 9406–9424, 1997.

Dubovik, O. and King, M. D.: A flexible inversion algorithm for retrieval of aerosol optical properties from Sun and sky radiance measurements, *J. Geophys. Res.*, 105, 20673–20696, 2000.

Fotiadi, A., Hatzianastassiou, N., Drakakis, E., Matsoukas, C., Pavlakis, K. G., Hatzidimitriou, D., Gerasopoulos, E., Mihalopoulos, N., and Vardavas, I.: Aerosol physical and optical properties in the Eastern Mediterranean Basin, Crete, from Aerosol Robotic Network data, *Atmos. Chem. Phys.*, 6, 5399–5413, doi:10.5194/acp-6-5399-2006, 2006.

Gerasopoulos, E., Amiridis, V., Kazadzis, S., Kokkalis, P., Eleftheratos, K., Andreae, M. O., Andreae, T. W., El-Askary, H., and Zerefos, C. S.: Three-year ground based measurements of aerosol optical depth over the Eastern Mediterranean: the urban environment of Athens, *Atmos. Chem. Phys.*, 11, 2145–2159, doi:10.5194/acp-11-2145-2011, 2011.

Hansen, J. E. and Travis, L. D.: Light scattering in planetary atmospheres, *Space Sci. Rev.*, 16, 527–610, doi:10.1007/BF00168069, 1974.

Hansen, J., Nazarenko, L., Ruedy, R., Sato, M., Willis, J., Del Genio, A., Koch, D., Lacis, A., Lo, K., Menon, S., Novakov, T., Perlwitz, J., Russell, G., Schmidt, G. A., and Tausnev, N.: Earth's energy imbalance: confirmation and implications, *Science*, 308, 1431–1435, doi:10.1126/science.1110252, 2005.

Holben, B. N., Eck, T. F., Slutsker, I., Tanre, D., Buis, J. P., Setzer, A., Vermote, E., Reagan, J. A., Kaufman, Y., Nakajima, T., Lavenu, F., Jankowiak, I., and Smirnov, A.: AERONET – a federated instrument network and data archive for aerosol characterization, *Remote Sens. Environ.*, 66, 1–16, 1998.

IPCC: Climate Change 2007 – The Physical Science Basis: Contribution of the Working Group I to the Fourth Assessment Report of the IPCC, Cambridge University Press, New York, NY, USA, 2007.

McArthur, L. J. B., Halliwell, D. H., Niebergall, O. J., O'Neill, N. T., Slusser, J. R., and Wehrli, C.: Field comparison of network sunphotometers, *J. Geophys. Res.*, 108, 4596, doi:10.1029/2002JD002964, 2003.

## Aerosol microphysical retrievals from PFR and AERONET

S. Kazadzis et al.

Title Page

Abstract

Introduction

Conclusions

References

Tables

Figures

◀

▶

◀

▶

Back

Close

Full Screen / Esc

Printer-friendly Version

Interactive Discussion



- Smirnov, A., Holben, B. N., Eck, T. F., Dubovik, O., and Slutsker, I.: Cloud screening and quality control algorithms for Aeronet database, *Remote Sens. Environ.*, 73, 337–349, 2000.
- Thomason, L. W. and Osborn, M. T.: Lidar conservation parameters derived from SAGE II extinction measurements, *Geophys. Res. Lett.*, 19, 1655–1658, 1992.
- 5 Twomey, S.: *Introduction to the Mathematics of Inversion in Remote Sensing and Linear Measurements*, Elsevier, New York, 1977.
- Veselovskii, I., Dubovik, O., Kolgotin, A., Korenskiy, M., Whiteman, D. N., Allakhverdiev, K., and Huseyinoglu, F.: Linear estimation of particle bulk parameters from multi-wavelength lidar measurements, *Atmos. Meas. Tech.*, 5, 1135–1145, doi:10.5194/amt-5-1135-2012, 2012.
- 10 Wehrli, C.: GAWPFR: a network of aerosol optical depth observations with precision filter radiometers, in: *WMO/GAW Experts Workshop on a Global Surface Based Network for Long Term Observations of Column Aerosol Optical Properties*, GAW Report No. 162, WMO TD No. 1287, 2005.
- 15 WMO: *WMO/GAW Experts workshop on a global surface-based network for long term observations of column aerosol optical properties*, (Davos, Switzerland, 8-10 March 2004), (WMO TD No. 1287), 153 pp., November 2005 (available at ftp://ftp.wmo.int/Documents/PublicWeb/arep/gaw/gaw162.pdf), 2005.

## Aerosol microphysical retrievals from PFR and AERONET

S. Kazadzis et al.

Title Page

Abstract

Introduction

Conclusions

References

Tables

Figures

◀

▶

◀

▶

Back

Close

Full Screen / Esc

Printer-friendly Version

Interactive Discussion



**Table 1.** Parameters of two types of particle size distribution used in the numerical simulations.

| Type | $r_f$ | $r_c$ | $\ln \sigma$ | $N_f/N_c$ |
|------|-------|-------|--------------|-----------|
| I    | 0.1   | 1.0   | 0.4          | $10^4$    |
| II   | 0.1   | 1.0   | 0.4          | $10^2$    |

## Aerosol microphysical retrievals from PFR and AERONET

S. Kazadzis et al.

**Table 2.** Uncertainties of effective radius  $\varepsilon_{\text{Reff}}$  and volume concentration  $\varepsilon_V$  retrieval for Type I and II PSDs.

| Input errors, % | $\varepsilon_{\text{Reff}}$ , % |         | $\varepsilon_V$ , % |         |
|-----------------|---------------------------------|---------|---------------------|---------|
|                 | Type I                          | Type II | Type I              | Type II |
| 0               | 20                              | 30      | 10                  | 50      |
| 5               | 40                              | 50      | 15                  | 60      |
| 10              | 50                              | 60      | 25                  | 65      |

Title Page

Abstract

Introduction

Conclusions

References

Tables

Figures

◀

▶

◀

▶

Back

Close

Full Screen / Esc

Printer-friendly Version

Interactive Discussion



**Aerosol  
microphysical  
retrievals from PFR  
and AERONET**

S. Kazadzis et al.

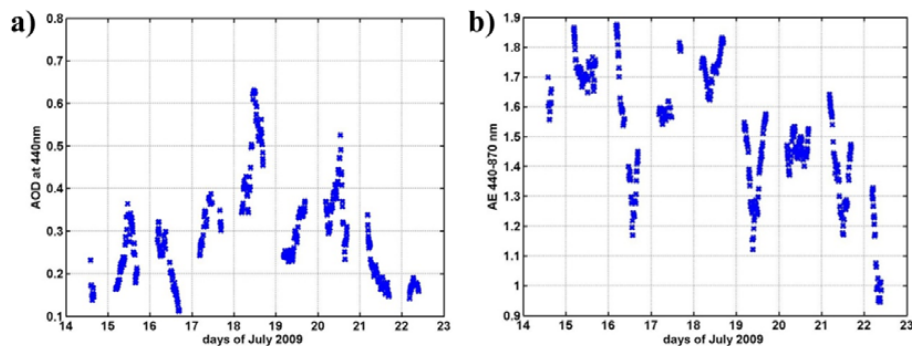


**Fig. 1.** (a) AOD at 440 nm and (b) the AE at 440–870 nm as monitored over Athens by the GAW-PFR instrument.

[Title Page](#)[Abstract](#)[Introduction](#)[Conclusions](#)[References](#)[Tables](#)[Figures](#)[⏪](#)[⏩](#)[◀](#)[▶](#)[Back](#)[Close](#)[Full Screen / Esc](#)[Printer-friendly Version](#)[Interactive Discussion](#)

**Aerosol  
microphysical  
retrievals from PFR  
and AERONET**

S. Kazadzis et al.

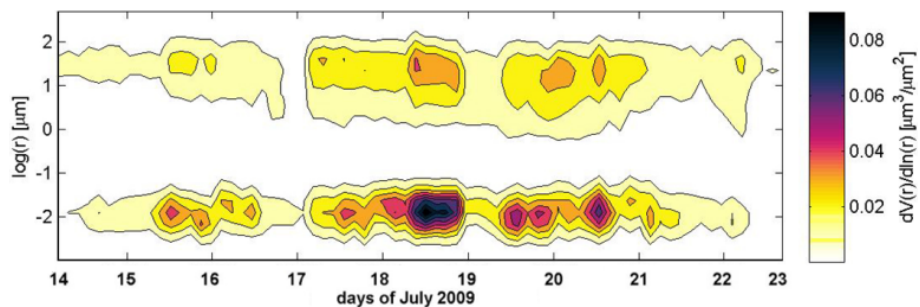


**Fig. 2.** Aerosol size distribution provided by the AERONET Level 2 Version 2 inversion.

[Title Page](#)[Abstract](#)[Introduction](#)[Conclusions](#)[References](#)[Tables](#)[Figures](#)[⏪](#)[⏩](#)[◀](#)[▶](#)[Back](#)[Close](#)[Full Screen / Esc](#)[Printer-friendly Version](#)[Interactive Discussion](#)

## Aerosol microphysical retrievals from PFR and AERONET

S. Kazadzis et al.

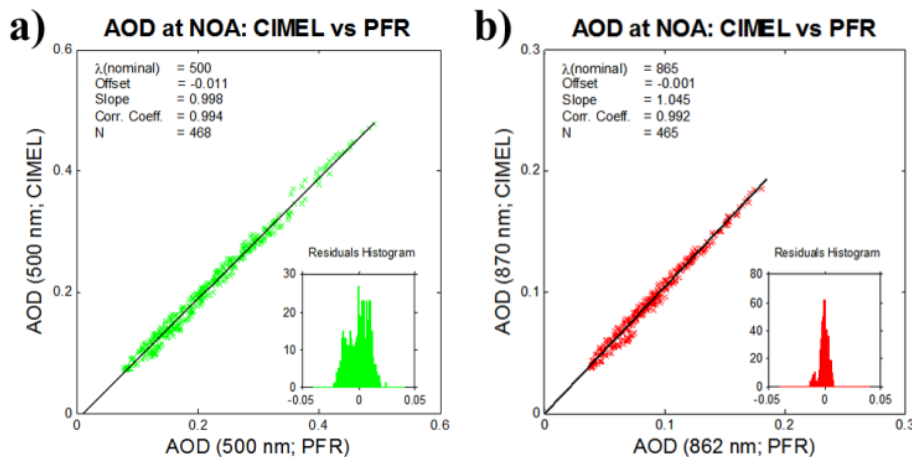


**Fig. 3.** Comparison of direct sun AODs from CIMEL and PFR at **(a)** 500 nm and **(b)** 865 nm for the whole measurement period. The plots inset present the histogram of residual values after the regression analysis.

Title Page

Abstract

Introduction

Conclusions

References

Tables

Figures

◀

▶

◀

▶

Back

Close

Full Screen / Esc

Printer-friendly Version

Interactive Discussion

Aerosol  
microphysical  
retrievals from PFR  
and AERONET

S. Kazadzis et al.

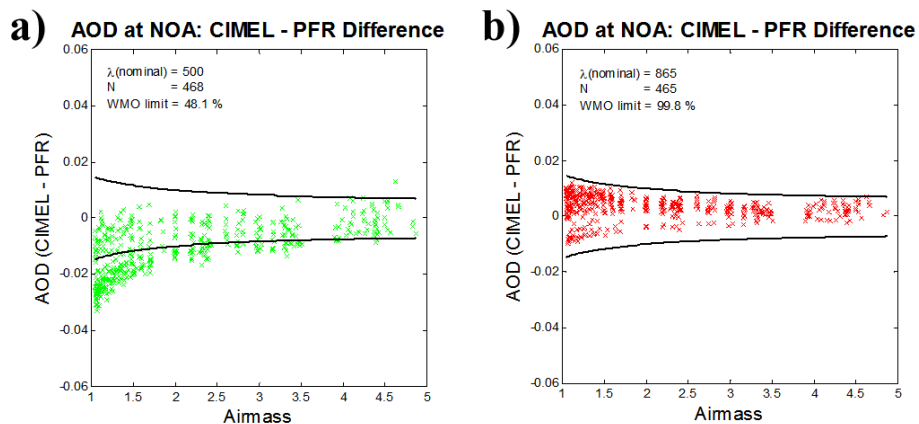


**Fig. 4.** AOD difference (CIMEL-PFR) vs. airmass at NOA illustrating the WMO criteria for traceability (solid line) at **(a)** 500 nm (green) and **(b)** 865 nm (red).

[Title Page](#)[Abstract](#)[Introduction](#)[Conclusions](#)[References](#)[Tables](#)[Figures](#)[◀](#)[▶](#)[◀](#)[▶](#)[Back](#)[Close](#)[Full Screen / Esc](#)[Printer-friendly Version](#)[Interactive Discussion](#)

**Aerosol  
microphysical  
retrievals from PFR  
and AERONET**

S. Kazadzis et al.

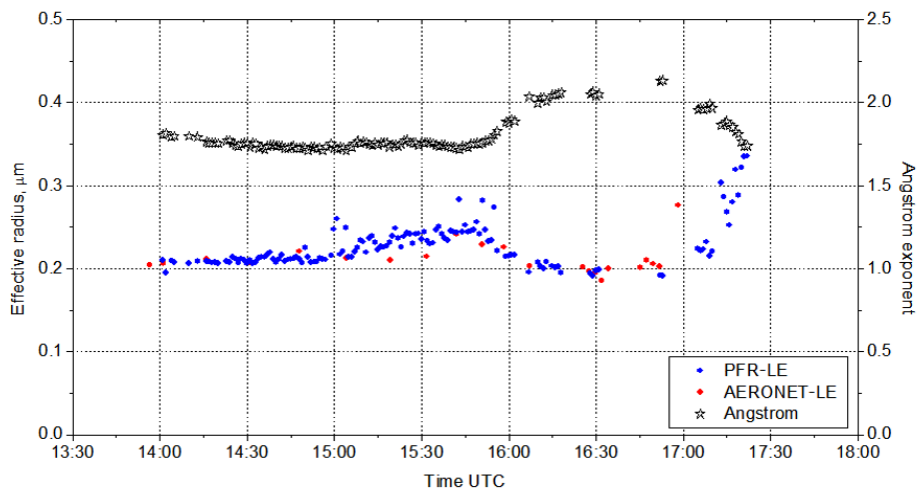


**Fig. 5.** Retrievals of the effective radius for the 14 July calculated from PFR (blue) and CIMEL AERONET (red) direct sun data using the LE method. Also shown is the CIMEL AERONET Angstrom exponent (black stars).

**Aerosol  
microphysical  
retrievals from PFR  
and AERONET**

S. Kazadzis et al.

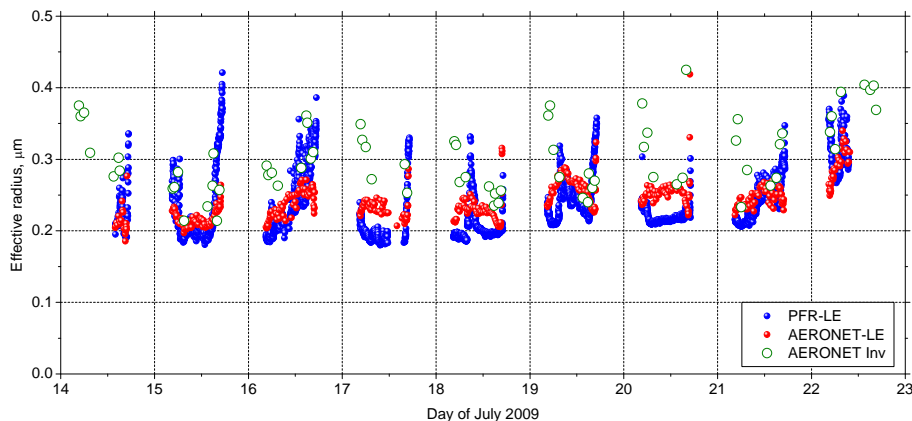


**Fig. 6.** Time series of the effective radius during the measurement period calculated by the PFR (blue=1 min resolution) and CIMEL AERONET (green=15 min resolution on average) using the LE method. Also shown is the value obtained from the AERONET Level 2 Version 2 inversion algorithm (red=8 times per day).

Title Page

Abstract

Introduction

Conclusions

References

Tables

Figures

◀

▶

◀

▶

Back

Close

Full Screen / Esc

Printer-friendly Version

Interactive Discussion

**Aerosol  
microphysical  
retrievals from PFR  
and AERONET**

S. Kazadzis et al.

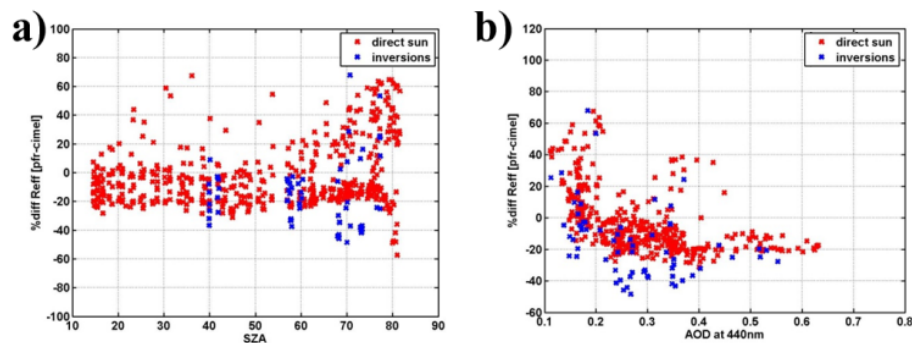


**Fig. 7.** (a) Percentage difference (PFR-CIMEL) of  $R_{\text{eff}}$  calculated from direct sun data using the LE method (red) together with the AERONET Level 2 Version 2 Inversion (blue) both as a function of solar zenith angle (SZA). (b) Percentage difference (PFR-CIMEL) of  $R_{\text{eff}}$  calculated from direct sun data using the LE method (red) and the AERONET Level 2 Version 2 Inversion (blue) both as a function of AOD.

**Aerosol  
microphysical  
retrievals from PFR  
and AERONET**

S. Kazadzis et al.

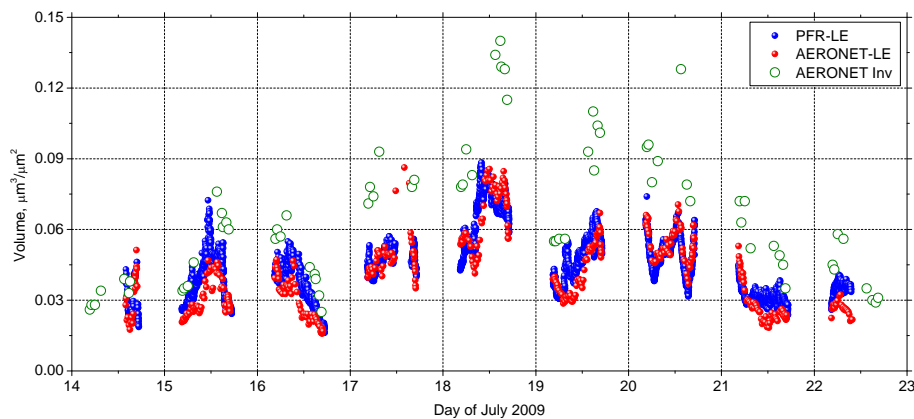


**Fig. 8.** Time series of the volume concentration  $V_c$  during the measurement period calculated by the PFR-LE (blue), the AERONET-LE (red) and the AERONET inversion algorithm (green).

Title Page

Abstract

Introduction

Conclusions

References

Tables

Figures

◀

▶

◀

▶

Back

Close

Full Screen / Esc

Printer-friendly Version

Interactive Discussion

## Aerosol microphysical retrievals from PFR and AERONET

S. Kazadzis et al.

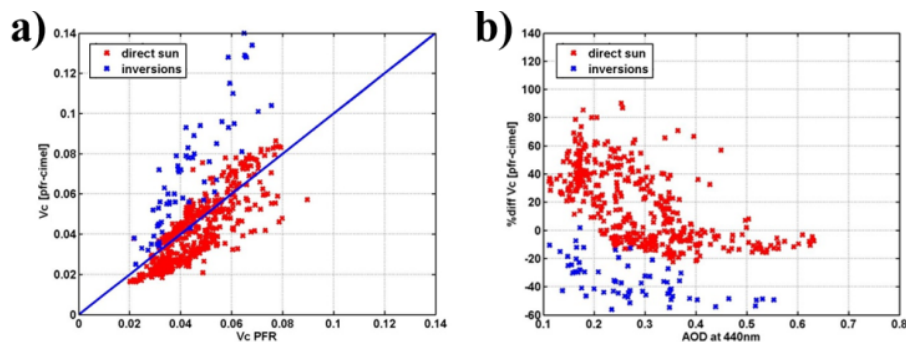


**Fig. 9.** (a) Scatter plot of  $V_c$  from PFR minus CIMEL (red) using direct sun data and the LE method and  $V_c$  from PFR minus the AERONET Level 2 Version 2 inversion (blue) as a function of  $V_c$  calculated from PFR-LE over the measurement period. (b): Percentage difference (PFR-CIMEL) of  $V_c$  calculated from direct sun data using the LE method (red) and with the AERONET Level 2 Version 2 Inversion (blue) both as a function of AOD.

Title Page

Abstract

Introduction

Conclusions

References

Tables

Figures

◀

▶

◀

▶

Back

Close

Full Screen / Esc

Printer-friendly Version

Interactive Discussion

Aerosol  
microphysical  
retrievals from PFR  
and AERONET

S. Kazadzis et al.

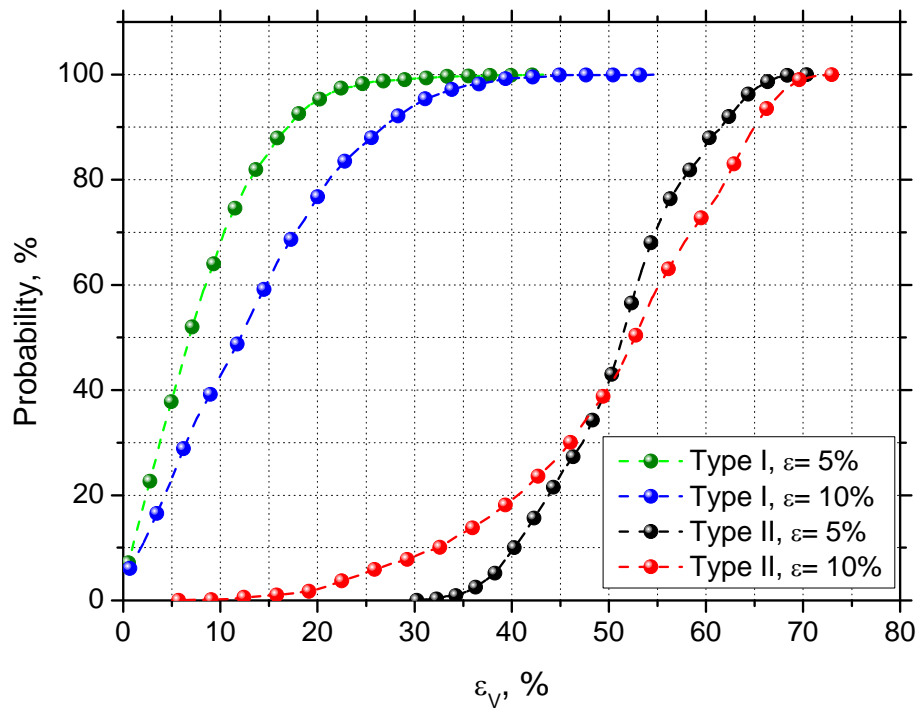


**Fig. 10.** Cumulative probability of the uncertainty  $\varepsilon_v$  in the volume concentration retrieval from the PFR data set with input errors  $\varepsilon = 5\%$  and  $10\%$  for Type I and Type II PSDs.



**Fig. 11.** The IAASARS/NOA meteorological station in Athens.

# AMTD

7, 99–130, 2014

## Aerosol microphysical retrievals from PFR and AERONET

S. Kazadzis et al.

Title Page

Abstract

Introduction

Conclusions

References

Tables

Figures

◀

▶

◀

▶

Back

Close

Full Screen / Esc

Printer-friendly Version

Interactive Discussion

